JOURNAL OF MATERIALS SCIENCE, 32 (1997) 5603–5610

Fe–Zn phase formation in interstitial-free steels hot-dip galvanized at 450 °C

Part II *0.20 wt % Al–Zn baths*

C. E. JORDAN, A. R. MARDER
Department of Materials Science and Engineering, Lehigh University, Bethlehem, PA 18015, USA

The effect of solute additions of titanium, titanium and niobium and phosphorus on interstitial-free steels on Fe–Zn phase formation after immersion in a 0.20 wt % Al–Zn bath was studied to determine the morphology and kinetics of the individual Fe–Zn phases formed. These results were contrasted to the previous study using a pure zinc (0.00 wt % Al) bath in Part I. It was found that in the 0.20 wt % Al–Zn bath, an iron–aluminide inhibition layer prevented uniform attack of the steel substrate. Instead, localized Fe–Zn phase growth occurred, termed outbursts, containing a two-phase layer morphology. Delta-phase formed first, followed by gamma-phase. Zeta-phase did not form in the 0.20 wt % Al–Zn bath, in contrast with zeta-phase formation in the pure zinc bath. As in the pure zinc bath, the growth kinetics of the total layer was controlled by the Fe–Zn phase in contact with the liquid zinc during galvanizing. For the 0.20 wt % Al–Zn bath, the Fe–Zn phase in contrast with the liquid zinc was the delta-phase, whereas the zeta-phase was in contact with liquid zinc in the pure zinc bath. The delta-phase followed $t^{1/2}$ parabolic growth, while the gamma-phase showed essentially no growth after its initial formation. Titanium and titanium + niobium solute additions, which enhance grain-boundary reactivity, resulted in more rapid growth kinetics of the gamma- and delta-phases. Phosphorus additions, which decrease grain-boundary reactivity, generally increased the incubation time and retarded the growth rate of the gamma-phase. These results further confirm the concept that solute grain-boundary reactivity is primarily responsible for Fe–Zn phase growth during galvanizing in a liquid Zn–Al bath in which an iron aluminide inhibition layer forms prior to Fe–Zn phase formation.

1. Introduction

Part I [1] reported a study of the effect of solute additions of titanium, titanium + niobium and phosphorus in interstitial free (IF) steels on the morphology and reaction kinetics of Fe–Zn phases formed during immersion in a pure Zn (0.00 wt % Al) liquid bath. These results showed that in aluminium-free zinc baths, uniform attack of the substrate steel developed a three-phase Fe–Zn alloy layer containing gamma-, delta- and zeta-phases. It was found that the gamma-layer growth kinetics was only affected by phosphorus additions, while zeta- and delta-phases were unaffected by any of the solutes studied. Both the zeta-phase layer and delta-phase layer followed a two-stage growth process, with their growth governed by $t^{1/3}$ and $t^{1/2}$ kinetics, respectively. The gamma-phase layer grew according to $t^{1/4}$ kinetics, indicative of grain-boundary diffusion-controlled growth. However, in automotive zinc coatings, most zinc baths contain deliberate additions of aluminium to form an $Fe_2Al_5(Zn)$ inhibition layer to prevent Fe–Zn intermetallic phase growth in the galvanized coating [2, 3]. The inhibition layer provides an incubation time in which Fe–Zn phase formation does not occur, and thus provides important processing control during immersion in the zinc pot [4]. It was the purpose of this study to evaluate systematically the effect of IF steel solute additions on the morphology and kinetics of Fe–Zn phase growth in a 0.20 wt % Al–Zn liquid bath at 450 °C.

2. Experimental procedure

The steel alloy materials used for this study were produced by BHP Steel in Port Kembla, Australia, and had the initial ingot compositions listed in Table I. All the alloys were cold rolled to a final sheet thickness of 0.4 mm (84% cold worked). Each 0.4 mm sheet sample (3.8 cm × 25.4 cm) was recrystallization annealed in a tube furnace under a reducing wet 18% H_2–N_2 gaseous atmosphere at 815 °C for 15 min. After annealing, the samples were water quenched and prepared for galvanizing. The final carbon content of the annealed sheet samples (Table II) was determined

0022–2461

TABLE I BPH sheet steel chemical analysis (10^{-4} wt %, or parts per million)

Steel alloy	C	Si	S	N	Al	Mn	P	Ti	Nb	B
LC	90	30	40	12	380	2580	20	80	< 50	< 3
LC–P	50	20	40	9	340	2690	600	60	< 50	< 3
TI IF	80	20	30	12	310	2590	30	750	< 50	< 3
Ti–P IF	60	50	20	10	390	2670	750	610	< 50	< 3
Ti–Nb IF	70	30	30	8	310	2470	40	330	210	< 3
Ti–Nb–P IF	60	50	30	9	330	2740	700	370	220	< 3

TABLE II Carbon and excess titanium (Ti**) content of IF steels after recrystallization annealing

Sample	Carbon content (wt %)	Ti**[a] (wt%)
LC (ULC)	0.003	− 0.0171
LC–P (ULC–P)	0.003	− 0.1080
TI IF	0.006	+ 0.0378
Ti–P IF	0.004	− 0.0776
Ti–Nb–IF	0.003	+ 0.0286
Ti–Nb–P IF	0.004	− 0.0730

Ti** = total Ti–3.99C–1.49S–3.42N–1.55P.

by inert gas fusion chemical analysis. The average grain sizes of all the alloys was in the range of 10–20 μm.

The laboratory hot-dip galvanizing process has been detailed elsewhere [1, 5]. In these experiments, hot-dip galvanizing was conducted at 450 °C in a 0.20 wt % Al–Zn bath saturated with iron at 0.008 wt %. The equilibrium solubility of iron (0.008 wt %) in a 0.20 wt % Al–Zn bath at 450 °C was previously determined by Tang *et al.* [6]. The light optical microscopy technique has been previously detailed [7] and the quantitative image analysis procedure was reported in Part I [1].

3. Results and discussion

3.1. Morphology of Fe–Zn phase formation in a 0.20 wt % Al–Zn bath

Fe–Zn phase growth was morphologically similar on all of the substrate steels studied, and a representative example of Fe–Zn alloy layer development on the Ti IF steel is shown in Fig. 1. The Fe–Zn phase layer development is also shown schematically in Fig. 2, where the sequence of reaction is represented chronologically. t_0 corresponds to zero time, and development occurs according to time such that $t_0 < t_1 < t_2 < t_3 < t_4$. Unlike the 0.00 wt % Al–Zn bath, total Fe–Zn alloy layer growth in the 0.20 wt % Al–Zn bath was inhibited by the initial formation of an Fe–Al intermetallic layer at the steel/coating interface (t_1 in Fig. 2), documented by other investigators to be either an Fe_2Al_5 phase [2] or an Fe–Zn–Al ternary compound [3]. The nature of this inhibiting layer is a transient one, and it is eventually penetrated by liquid zinc to form localized growth of Fe–Zn delta-phase (t_2) and after some incubation time, gamma-phase (t_3). The localized growths (outbursts) eventually coalesce to form regions of a continuous Fe–Zn alloy layer; however, areas of Fe_2Al_5 inhibition layer remain undisturbed up to 300 s reaction time (t_4). Therefore, the localized Fe–Zn growth reaction is due to the inhibiting effect of an Fe_2Al_5(Zn) layer that first forms at the steel/coating interface and acts as a physical barrier to zinc diffusion, resulting in discontinuous Fe–Zn alloy phase growth in a 0.20 wt % Al–Zn bath.

Localized regions of Fe–Zn growth (outburst) at the steel/coating interface were seen on all of the steel substrates studied. The localized regions of Fe–Zn growth showed a two-phase layer morphology within the total Fe–Zn alloy reaction layer, with delta phase layer forming first at the steel/coating interface, followed by gamma-phase layer formation at the alpha-iron/delta-phase interface. The delta-phase was found to form at the shortest reaction time of 5 s, and was the dominant growth layer within the total Fe–Zn alloy layer at all of the reaction times studied.

In order to confirm the individual phase-layer identification initially characterized by morphology in light optical microscopy (LOM), electron probe microanalysis for iron, zinc and aluminium composition was determined at 1.0 μm increments across the total Fe–Zn alloy layer perpendicular to the steel/coating interface (parallel to the direction of diffusion) for the 10, 60 and 300 s immersion samples. An example of the iron and aluminium concentration profile data is plotted for the Ti IF substrate in Fig. 3, and supports the gamma- and delta-phase identification and morphology determined by LOM. Because delta-phase has a high solubility for aluminium [8], aluminium present at the steel/coating interface becomes distributed throughout the delta-phase layer. All of the substrate steels showed similar iron and aluminium concentration profiles. Thus, the composition analysis determined in this study did not support the work of Fukuzuka *et al.* [9], who had previously reported that IF steels galvanized in aluminium containing baths had lower amounts of aluminium located at the steel/coating interface, and that this lack of aluminium resulted in the observed higher reactivity of IF steels. An example of a back-scattered electron (BSE) image of an 0.20 wt % Al–Zn coating is shown in Fig. 4. The atomic number contrast in the image also indicates a two-phase layer morphology in the localized Fe–Zn growth regions. The BSE images confirmed that no zeta-phase layer formed, as was observed in LOM and determined from compositional data analysis of the Fe–Zn alloy layer.

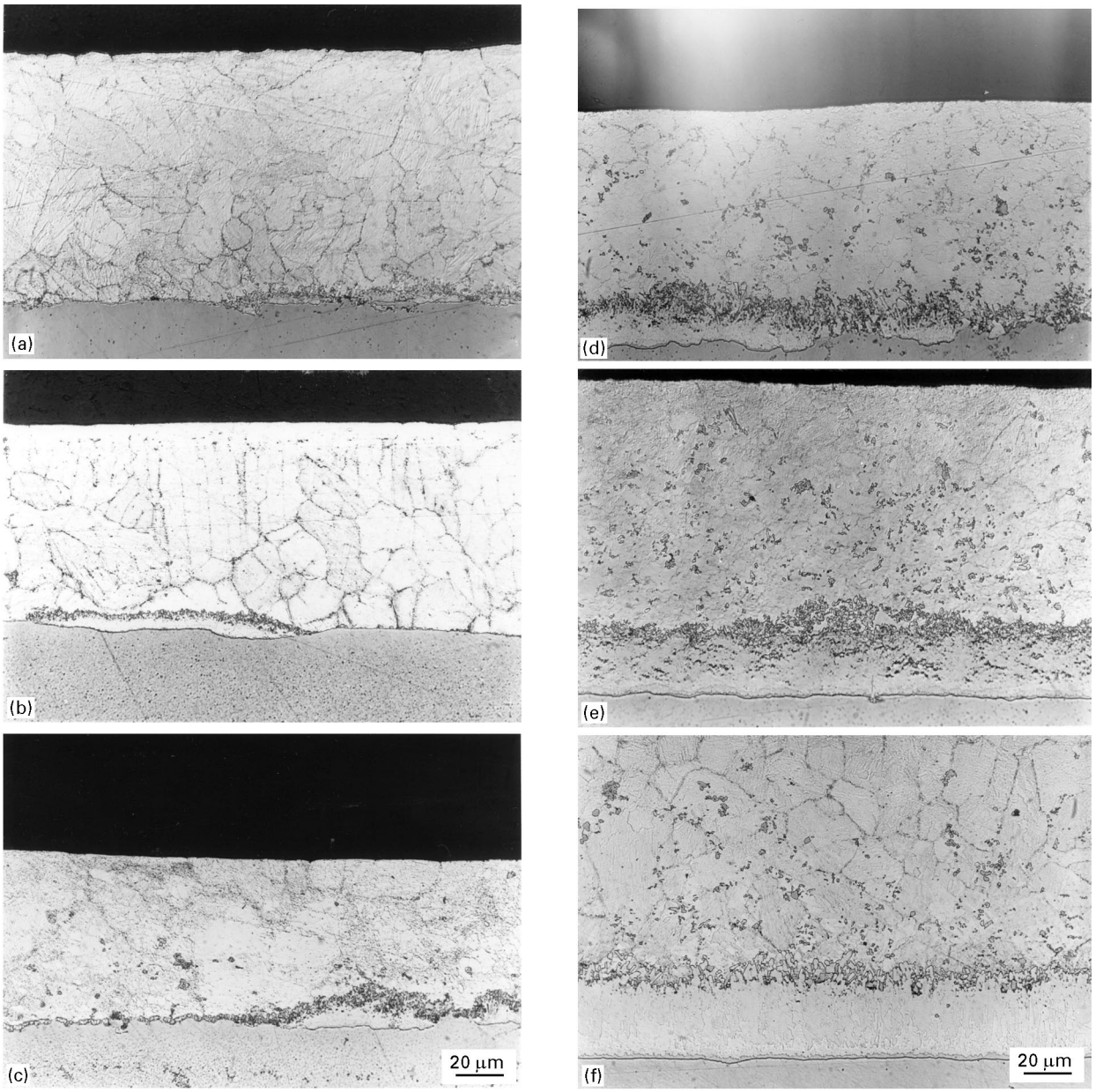

Figure 1 Ti IF steel hot-dip galvanized in a 0.20 wt % Al–Zn bath for (a) 5 s, (b) 10 s, (c) 30 s, (d) 60 s, (e) 120 s, and (f) 300 s.

In contrast to the 0.00 wt % Al–Zn bath, zeta-phase was not detected in the coatings formed in the 0.20 wt% Al–Zn bath because the diffusion path for the Fe–Zn reaction layer through the metastable ternary Fe–Zn–Al isotherm at 450 °C [8] indicates that the delta-phase is in equilibrium with eta-phase, the solid solution of iron in zinc. The equilibrium ternary phase diagram at 450 °C (e.g. [10]) would have led to the incorrect identification of delta- and zeta-phases within the total Fe–Zn alloy layer. The metastable ternary diagram (shown in Fig. 5) is a more accurate guide to the identification of phase layers that form after short-term reactions (< 30 min). The diffusion path through the ternary isotherm (determined from composition analysis of the total Fe–Zn alloy layer after 300 s immersion in a 0.20 wt % Al–Zn bath) follows a path that does not allow for the formation of the zeta-phase. The diffusion path for the Fe–Zn reaction layer remained the same over 10–300 s reaction time indicating diffusional growth of the Fe–Zn phases during immersion in the 0.20 wt % Al–Zn bath. The Fe–Al inhibition layer was too thin to be evaluated by electron microprobe analysis for composition. The diffusion path for the Fe–Zn reaction layer (starting from the iron corner of the ternary diagram) was determined to follow an $\alpha/(\alpha + \Gamma)/\Gamma/(\Gamma + \delta)/\delta/(\delta + \eta)/\eta$ path, and the $(\Gamma + \delta)/\delta/(\delta + \eta)/\eta$ portion of the path is shown in Fig. 5.

The morphology of the localized Fe–Zn growths also supports the finding that delta-phase is in metastable equilibrium with eta-phase. Fig. 6 shows a morphology referred to as a "breakaway morphology." The "breakaway morphology" has a mottled appearance because it has been penetrated by liquid zinc and contains regions of entrapped eta-phase; therefore, the delta-phase layer is in a state of metastable equilibrium with liquid zinc during immersion. The penetration of zinc through the Fe–Zn phase in contact with the melt was also found to occur for the zeta-phase layer in the 0.00 wt % Al–Zn bath [1]. The zeta layer

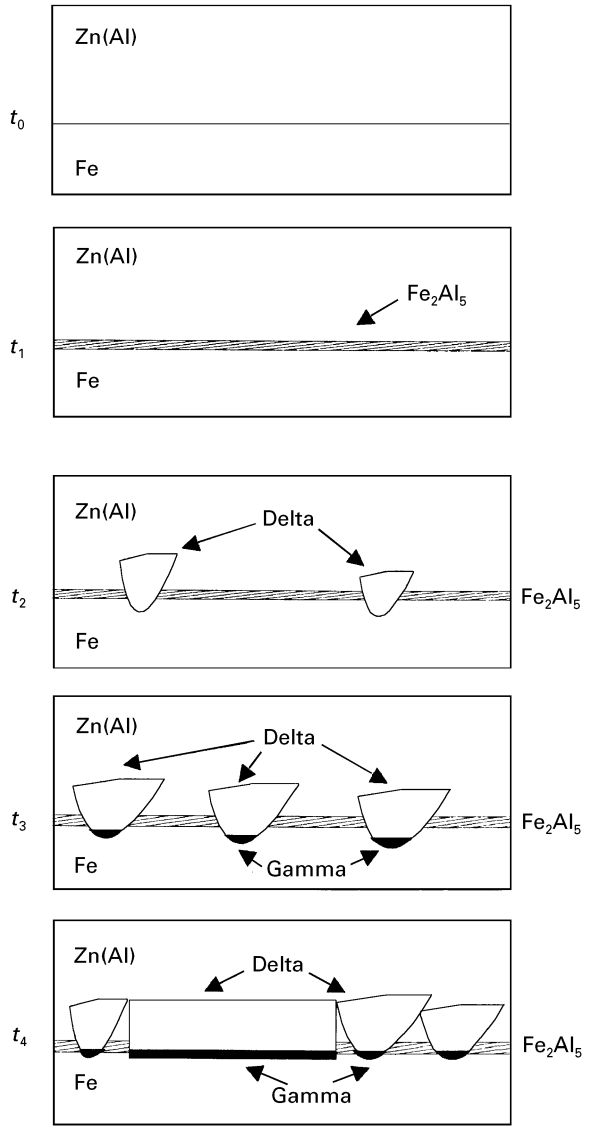

Figure 2 A schematic representation of Fe–Zn phase layer formation in a 0.20 wt % Al–Zn galvanizing bath. t_0 corresponds to zero time, and development occurs according to time, such that $t_1 < t_2 < t_3 < t_4$.

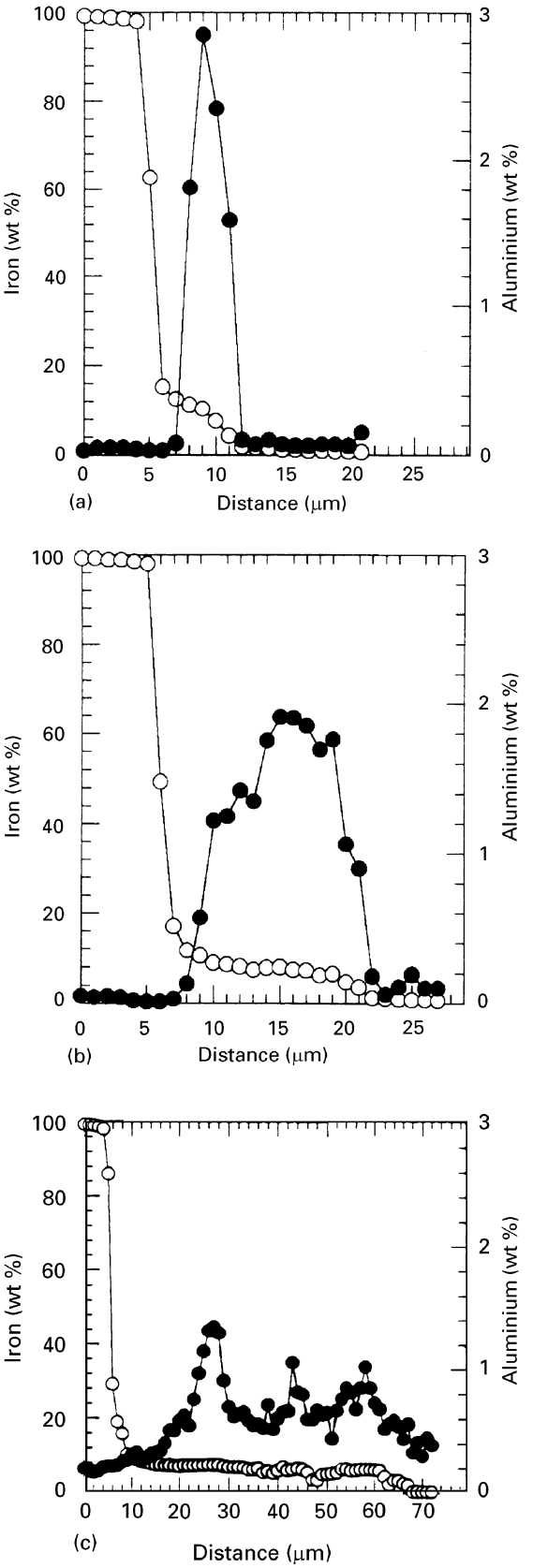

Figure 3 (○) Iron and (●) aluminium concentration profiles for the total Fe–Zn alloy layer formed on the Ti IF steel hot-dip galvanized in a 0.20 wt % Al–Zn bath for (a) 10 s, (b) 60 s, and (c) 300 s.

also showed regions of entrapped eta-phase, representative of liquid zinc penetration and subsequent solidification. In the 0.00 wt % Al–Zn bath, zeta-phase was in a state of metastable equilibrium with the zinc melt during immersion.

The growth of the delta-phase was rapid and was most likely due to liquid zinc penetration of the delta-phase which resulted in a porous structure (or breakaway morphology) when observed in cross-section (Fig. 6). After an incubation time, gamma-phase formed at the alpha-iron/delta-phase interface. The gamma-phase kinetics were difficult to define according to a growth–time relationship due to little or no growth. As in the case of the 0.00 wt % Al–Zn coatings, the gamma-phase was found to disappear on the phosphorus-containing steels after 300 s reaction [1].

3.2. Kinetics of the Fe–Zn phase growth in a 0.20 wt % Al–Zn bath

The same substrate steel alloys studied in the 0.00 wt % Al–Zn bath [1] were also analysed for galvanizing reaction kinetics for 5–300 s reaction time in a 0.20 wt % Al–Zn bath. Total alloy layer growth and individual gamma- and delta-phase layer growth were characterized at localized regions of Fe–Zn phase growth along the steel/coating interface. Total

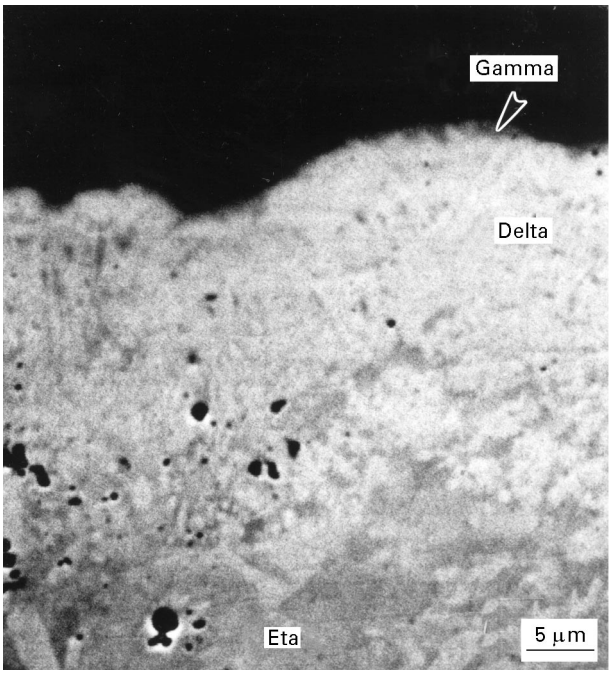

Figure 4 BSE image of the two distinct Fe–Zn phase layers formed on the 15 μm grain size ULC steel hot-dip galvanized in a 0.20 wt % Al–Zn bath for 300 s immersion.

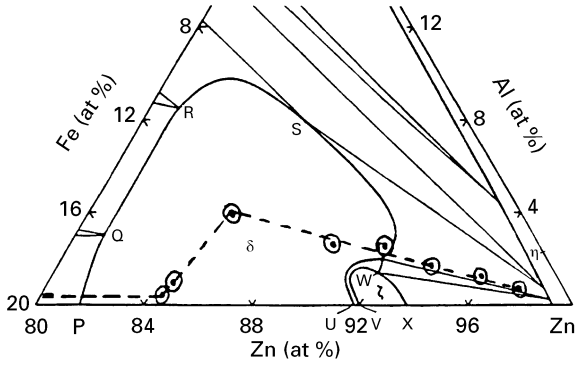

Figure 5 Diffusion path of the Fe–Zn alloy layer formed in the 0.20 wt % Al–Zn bath of the metastable Fe–Zn–Al isotherm at 450 °C [3]. (a) Fe–Zn binary portion, (b) Zn-rich corner.

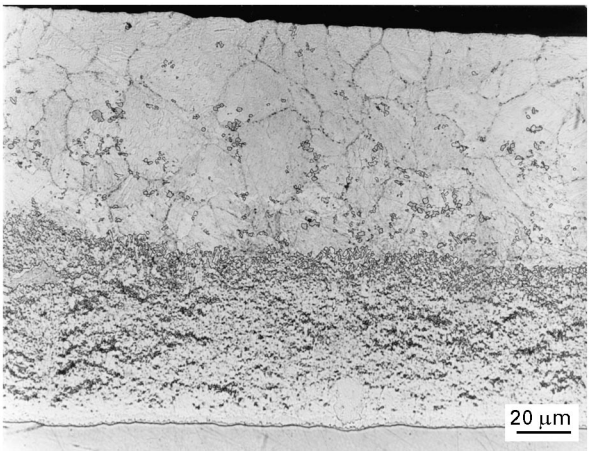

Figure 6 Ti IF steel hot-dip galvanized in a 0.20 wt % Al–Zn bath for 300 s immersion.

alloy layer thickness data for all of the substrate steels studied are shown in Fig. 7. The total alloy layer thickness data were first analysed to determine growth-rate time-constant, n, values and the total

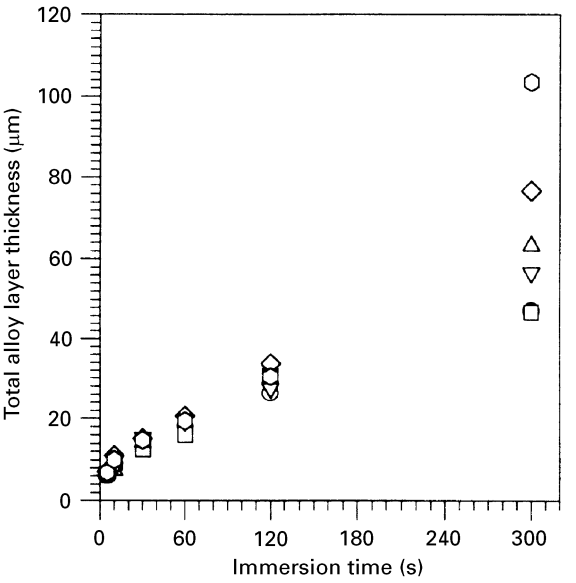

Figure 7 Total Fe–Zn alloy layer growth for substrate steels hot-dip galvanized in a 0.20 wt % Al–Zn bath: (○) ULC, (□) ULC–P, (△) Ti IF, (▽) Ti–P IF, (◇) Ti–Nb IF, (⬡) Ti–Nb–P IF.

TABLE III Total Fe–Zn alloy layer growth-rate time-constant, n, values for the steels hot-dip galvanized in a 0.20 wt % Al–Zn bath

Sample	Growth-rate time constant, n
ULC	0.42 ± 0.02
ULC–P	0.47 ± 0.05
Ti IF	0.55 ± 0.04
Ti–P IF	0.50 ± 0.04
Ti–Nb IF	0.54 ± 0.06
Ti–Nb–P IF	0.60 ± 0.09

alloy layer n values are reported in Table III. The n values range from 0.47–0.60, corresponding to parabolic kinetics, where $n = 0.50$. Up to 120 s reaction time all of the substrates followed the same outburst growth behaviour, and only at 300 s reaction were large differences in total growth of the outbursts observed between the substrates (Fig. 7). The breakaway morphology of the outburst was extremely pronounced on the Ti/Ti–P and Ti–Nb/Ti–Nb–P IF steel substrates at 300 s reaction, indicating a rapid change in the growth rate of the outburst. Because data were not available for reaction times longer than 300 s, this rapid growth of the outbursts observed on the IF steels could not be quantified.

Individual phase layers of gamma- and delta-phases were observed to develop for all of the steels hot-dip galvanized in the 0.20 wt % Al–Zn bath. Individual phase layer growth data for the separate substrate steel alloys were analysed; an example is shown in Fig. 8. The gamma-phase layer was observed to form first after different incubation times, depending upon substrate chemistry (see Table IV), which may be due to steel solute addition effecting the breakdown of the inhibition Fe_2Al_5 layer.

Phosphorus solute additions to the substrate steel in most cases delayed the onset of the gamma reaction.

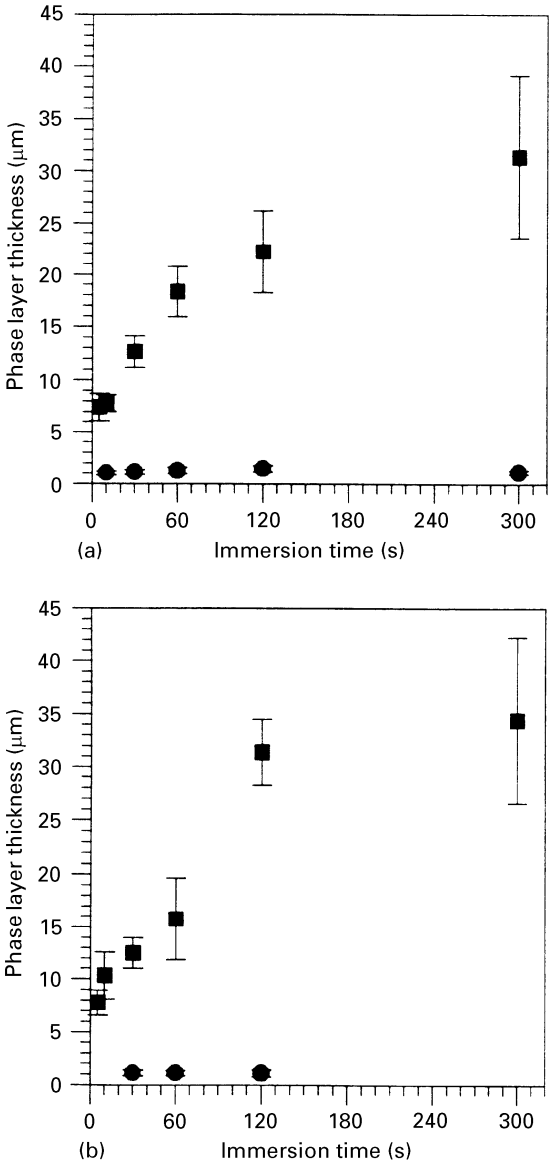

Figure 8 Individual Fe–Zn (●) gamma and (■) delta-phase layer growth for the (a) ULC and (b) ULC–P steel substrates hot-dip galvanized in a 0.20 wt % Al–Zn bath.

TABLE IV Reaction time at which the Fe–Zn gamma-phase layer was first observed to form and grow on steels hot-dip galvanized in a 0.20 wt % Al–Zn bath

Sample	Reaction time (s)
ULC	10
ULC–P	30
Ti IF	30
Ti–P IF	60
Ti–Nb IF	10
Ti–Nb–P IF	10

To evaluate best the gamma-phase layer data, growth-rate time-constant values were determined over the associated time frame at which gamma-phase was found to form and grow on the different steel substrates. The n values for the gamma layer are reported in Table V. A large degree of error was found to be associated with some of the values; however, the gamma layer generally was found to show little or no growth in the 0.20 wt % Al–Zn bath. The observed lack of growth of the gamma phase has been previously reported for galvanized coatings formed in a bath containing 0.10 wt % Al–Zn which were then annealed at temperatures of 450–550 °C [11]. Comparison of the non-phosphorus containing substrates (ULC, Ti IF and TiNb IF) indicates that titanium and titanium + niobium solute additions enhanced the growth kinetics (n value) of the gamma-phase layer.

TABLE V Individual Fe–Zn phase layer growth-rate time-constant, n, values for the steels hot-dip galvanized in a 0.20 wt % Al–Zn bath

Sample/layer	Growth-rate time constant, n
Gamma-phase layer	
ULC	0.050 ± 0.049
ULC–P	-0.032 ± 0.003
Ti IF	0.16 ± 0.01
Ti–P IF	-0.528[a]
Ti–Nb IF	0.19 ± 0.05
Ti–Nb–P IF	0.036 ± 0.158
Delta-phase layer	
ULC	0.38 ± 0.02
ULC–P	0.38 ± 0.05
Ti IF	0.53 ± 0.07
Ti–P IF	0.50 ± 0.07
Ti–Nb IF	0.57 ± 0.07
Ti–Nb–P IF	0.62 ± 0.09

[a] No error determined due to fit over just two data points.

Because all of the phosphorus-containing alloys did show the disappearance of the gamma-phase layer after 300 s reaction, a negative n value was determined for the growth-rate time constant on the ULC–P and Ti–P steel substrates (Table V). The negative n values are not physically possible; however, they do indicate a situation of no growth of the gamma-phase layer and its consumption over time by the delta-phase layer. Phosphorus additions to the substrate steel appeared, eventually over time to destabilize the interfacial gamma layer, probably by preventing further diffusion of zinc down substrate steel grain boundaries [12], as was found to occur in 0.00 wt % Al–Zn baths [1]. Toki *et al.* [13] suggest that grain-boundary reactivity can be related to the chemical composition of the steel as follows

$$\text{Ti}^{**} = \text{total Ti} - 3.99\text{C} - 1.49\text{S} - 3.42\text{N} - 1.55\text{P} \quad (1)$$

and is reported in Table II for the alloys studied in this investigation. A positive Ti** indicates excess titanium and therefore "clean" (carbide-free) and reactive grain boundaries. A negative value of Ti** would indicate that not all of the solute carbon is tied up and zinc diffusion down the boundaries would be blocked. Fig. 9 shows that alloys with positive Ti** have the highest gamma growth-rate time constants, n, indicating that these alloys are most reactive. (A negative growth-rate time constant is plotted as zero in this figure.) The phosphorus alloys with low Ti** slow gamma-layer formation, confirming that phosphorus

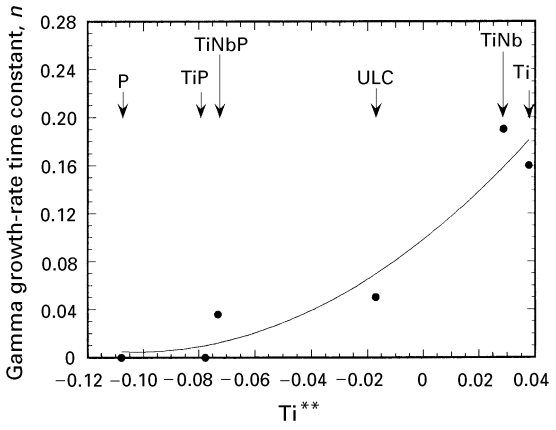

Figure 9 The effect of Ti** on the gamma growth-rate time constant, *n*.

solute additions segregate at the grain boundaries and prevent zinc reaction with the iron [12].

According to the growth-rate curves for all the substrates (e.g. Fig. 8), the delta layer formed on the ULC/ULC–P substrates followed parabolic growth up to 300 s reaction time, while the Ti/Ti–P and Ti–Nb/Ti–Nb–P steels showed parabolic growth up to 120 s reaction time. The observed growth behaviour was related to the accelerated rate of outburst growth which occurred on the titanium and titanium + niobium IF steel substrates. Delta-phase layer growth was first fit to determine growth-rate time-constant values. The Ti/Ti–P and Ti–Nb/Ti–Nb–P steel data were fit up to 120 s reaction time as growth at 300 s did not follow the growth behaviour which occur red at earlier reaction times. The *n* values are reported in Table V. The *n* values range from 0.38–0.62, indicating that the ULC/ULC–P steels had lower *n* values (0.38) than those for the titanium and titanium + niobium containing steels ($n = 0.5$–0.62). Therefore, delta layer growth followed more rapid kinetics on the Ti IF/Ti–P IF and Ti–Nb IF/Ti–Nb–P IF steels. As was found to occur for the gamma-phase layer growth, solute additions of titanium and titanium + niobium resulted in more rapid growth kinetics of the delta-phase layer. Additions of phosphorus were found not to influence the kinetics of delta layer growth for any of the steels studied.

Summarizing the Fe–Zn phase growth kinetics that occurred in the 0.20 wt % Al–Zn bath, it was found that the total Fe–Zn alloy that formed was a localized growth, due to the initial formation of an Fe–Al inhibition layer (Fe_2Al_5) upon immersion of the substrate into the zinc bath. The total Fe–Zn alloy or outburst followed $t^{1/2}$ growth kinetics, as was generally found for the delta-phase layer growth which was in contact with the liquid zinc melt during immersion. Similarly, in the 0.00 wt % Al–Zn bath, total Fe–Zn alloy layer growth followed a $t^{1/3}$ relationship as did the zeta-phase layer which was in contact with the liquid zinc during immersion in that bath [1]. Thus, the supply of zinc through the Fe–Zn phase in contact with the liquid zinc, dominates the overall total Fe–Zn alloy layer growth reaction. The fact that the *n* values for the total alloy layer are not the same for the 0.00 and 0.20 wt % Al–Zn baths is most likely related to the consumption of the zeta-phase layer by the rapidly growing delta layer in 0.00 wt % Al–Zn coatings.

The gamma-phase layer in the 0.20 wt % Al–Zn bath showed little or no growth, therefore, its growth kinetics were difficult to define. Solute additions to titanium and titanium + niobium were found to cause more rapid growth of both the gamma- and delta-phase layers in 0.20 wt % Al–Zn baths, while phosphorus solute additions resulted in "negative" growth kinetics of the gamma-phase layer, which led to the eventual disappearance of the layer at the longest time of reaction studied.

The previously reported effects of substrate solute additions on galvanizing have concentrated on reactions in zinc baths containing aluminium due to the fact that these baths are commonly used in the steel industry to produce high-quality automotive zinc coatings [4]. It is generally thought that phosphorus solute additions reduce steel reactivity while titanium additions increase steel reactivity during hot-dip galvanizing and galvannealing, thus affecting process control of an optimally allowed Fe–Zn coating. The findings of the present studies show that similar to the 0.00 wt % Al–Zn baths, phosphorus retards gamma layer growth in the 0.20 wt % Al–Zn baths and has no effect on delta layer phase growth or total Fe–Zn alloy layer growth. Unlike the 0.00 wt % Al–Zn baths, titanium and niobium additions to the substrate steel accelerated the growth kinetics of both the gamma- and delta-phase layers in the 0.20 wt % Al–Zn bath.

4. Conclusions

From this study of Fe–Zn phase formation in IF steels hot-dipped at 450 °C in a 0.2 wt % Al–Zn bath, the following conclusions can be drawn.

1. Discontinuous Fe–Zn phase growth (outburst formation) was observed at the steel/coating interface, due to the inhibition effect of an Fe–Al layer that first formed upon immersion of the substrate into the bath. A two-phase layer morphology developed within the localized Fe–Zn growth regions. Delta-phase was the first phase to form, followed by the formation of gamma-phase.

2. The growth kinetics of the total Fe–Zn alloy layer followed that of the delta-phase. Therefore, the Fe–Zn phase layer in contact with the liquid zinc during galvanizing (delta-phase, in this case) was found to control the growth kinetics of the total Fe–Zn alloy layer. The delta-phase followed $t^{1/2}$ parabolic growth, while the gamma-phase showed essentially no growth after its initial formation.

3. Substrate steel titanium and titanium + niobium solute additions resulted in more rapid growth kinetics of the gamma- and delta-phase layers. Phosphorus solute additions were also found to influence the incubation time for the formation of the gamma-phase. Phosphorus solute additions to ULC and Ti IF steels increased the incubation time for gamma-phase formation and retarded the growth-rate kinetics of the gamma-phase.

Acknowledgements

The authors thank A. O. Benscoter for his guidance in metallography. The helpful discussions with Professor M. Notis, Lehigh University, and Professor F. van Loo, Eindhoven Technical University, are gratefully acknowledged. In addition, the sponsorship of Cockerill Sambre (Michel Dubois), BHP Steel (Peter Mercer) and Union Miniere (Jean Wegria) is gratefully acknowledged.

References

1. C. E. JORDAN and A. R. MARDER, *J. Mater. Sci.* **32** (1997) 5603–5610.
2. J. S. KIRKALDY and M. UREDNICEK, *Z. Metallkde* **64** (1973) 899.
3. A. R. P. GHUMAN and J. I. GOLDSTEIN, *Metall. Trans.* **2A** (1971) 2903.
4. J. MACOWIAK and N. R. SHORT, *Int. Metals Rev.* **1** (1979) 1.
5. C. E. JORDAN and A. R. MARDER, "GALVATECH '95" edited by J.E. Hartmann (Iron and Steel Society, Warrendale, PA, 1995) p. 319.
6. N-Y. TANG, G. R. ADAMS and P. S. KOLISNYK, *ibid*., p. 777.
7. C. E. JORDAN, K. M. GOGGINS, A. O. BENSCOTER and A. R. MARDER, *Mater. Charact.* **31** (1993) 107.
8. P. PERROT, J-C. TISSIER and J-Y. DAUPHIN, *Z. Metallkde* **83** (1992) 11.
9. T. FUKUZUKA, M. URAI and K. WAKAYAMA, *Kobe Steel Engng. Rep.* **30** (1980) 77.
10. K. OSINSKI, Doctoral Thesis, Eindhoven, The Netherlands (1983).
11. C. E. JORDAN, K. M. GOGGINS and A. R. MARDER, *Metall. Mater. Trans.* **25A** (1994) 2101.
12. L. ALLEGRA, R. G. HART and H. E. TOWNSEND, *Metall. Trans.* **14A** (1983) 401.
13. T. TOKI, K. OSHIMA, T. NAKAMORI, Y. SAITO, T. TSUDA and Y. HOBO, in "The Physical Metallurgy of Zinc Coated Steel", edited by A. R. Marder (TMS, Warrendale, PA, 1994) p. 169.

Received 3 March
and accepted 29 May 1997